Penetration factor in deformed potentials: Application to α decay with deformed nuclei

M. Ismail, A. Y. Ellithi, and M. M. Botros
Department of Physics, Faculty of Science, Cairo University, Giza, Egypt

A. Abdurrahman
Department of Physics, Faculty of Engineering, Misr University for Science and technology (MUST), Giza, Egypt
(Received 11 July 2011; revised manuscript received 10 July 2012; published 16 October 2012)

A new averaging process of the calculation of α-decay half-lives for heavy and superheavy nuclei is studied in the framework of a deformed density-dependent cluster model. The potential between a spherical α particle and a deformed daughter nucleus is calculated numerically from the double-folding model by the multipole expansion method. The nuclear potential is calculated at each α-particle emission angle applying the Bohr-Sommerfeld condition at each case. The penetration factors and the half-lives for all the emission angles are evaluated with the new averaging process and compared with older values based on a fixed value of the nuclear potential depth. Finally**,** the half-lives of 83 even-even heavy nuclei in the atomic-number range 82–118 are calculated by the two methods and compared with their experimental values and the corresponding half-lives of the spherical daughter nuclei.

DOI: 10.1103/PhysRevC.86.044317 PACS number(s): 23.60.+e, 21.10.Tg

I. INTRODUCTION

Measurements on α decay can provide reliable information on nuclear structure, such as ground-state energy, lifetime, nuclear spin, and parity. α decay is now a powerful tool for investigating the details of nuclear structure, for example, α clustering, shell effects, effective nuclear interaction, and nuclear deformation [1–7].

A number of approaches were used to study the α-decay phenomenon; they are based on the shell model, fissionlike model, cluster model [8–14], and the coupled-channel approach, which has been used also in Ref. [15]. The density-dependent cluster model (DDCM) has been recently used by many authors [16–18] to calculate the half-life of α emission for heavy and superheavy nuclei. Because a large number of heavy and superheavy nuclei are deformed, it was natural to extend the DDCM calculations to deformed nuclei and some earlier steps in this direction had been taken [17,18]. In the present work, we discuss a new simple approach for taking the average values of some physical quantities over the orientation angles of α emission measured from the symmetry axis of the deformed daughter nucleus (briefly called *emission angle*), in the framework of the DDCM.

II. THE MODEL FORMALISM

In the DDCM model, the ground state of the parent nucleus is assumed to be a spherical α particle with Gaussian density distribution, as in Ref. [17], interacting with a deformed daughter nucleus (*core*) through the effective potential which consists of the nuclear U_{N}, Coulomb U_{C}, and centrifugal potentials [17–19],

$$U_{\mathrm{total}}(r,\beta)=\lambda(\beta)U_N(r,\beta)+U_C(r,\beta)+\frac{\hbar^2}{2\mu}\frac{(L+1/2)^2}{r^2}, \quad (1)$$

where r is the separation distance between the mass centers of the α particle and the core, β is the emission angle of the α particle, λ is a measure of the strength (depth) of the double-folding nuclear potential, and L is the angular momentum of the α particle. The nuclear and Coulomb potentials are obtained in the framework of the double-folding model [17,20], and the matter (or charge) density distribution of the daughter nucleus is assumed to be deformed Fermi distribution with half-density radius $R(\theta)$ given by

$$R(\theta)=R_\circ[1+\delta_2Y_{20}(\theta)+\delta_3Y_{30}(\theta)+\delta_4Y_{40}(\theta)]. \quad (2)$$

R_o and the diffuseness parameter a are taken as in Ref. [17].

The nucleon-nucleon interaction used in the present work is the M3Y-Reid potential [21,22]. For the spherical-deformed interacting pair, the double-folding potential is calculated numerically by using the multipole expansion method [17,22,23]

In the present work, we consider daughter nucleus with static quadrupole, octupole, and hexadecapole deformations and take the *dominant* form factors A_L^D; $L=0,1,2,3,4,5$ into account. If Q is the experimental α-decay energy [24], then by solving numerically the equation $U_{\mathrm{total}}(r,\beta)=Q$, one obtains the three classical turning points $r_1(\beta)$, $r_2(\beta)$, and $r_3(\beta)$ at each emission angle β in increasing order for the distance from the origin. The depth $\lambda(\beta)$ of the double-folding nuclear potential in Eq. (1) is determined separately for each emission angle of the α particle to ensure the quasibound Bohr-Sommerfeld (B-S) condition,

$$\int_{r_1(\beta)}^{r_2(\beta)}\sqrt{\frac{2\mu}{\hbar^2}|Q-U_{\mathrm{total}}(r,\beta)|}dr=(G-L+1)\frac{\pi}{2}, \quad (3)$$

where L is the angular momentum carried by the α particle and G is the global quantum number given in Ref. [25]; $G=20$ for the nuclei considered in the present work. Recently, some authors used the Wildermuth condition [26] instead of the B-S condition given by Eq. (3). It had been found that the two conditions differ slightly in the value of G ($G=22.5$ in the B-S condition compared with $G = 22$ in the Wildermuth condition).

According to the semiclassical theory, the α-decay width in the *deformed* DDCM is given by [17,18],

$$\Gamma = P_\alpha \frac{\hbar}{4\mu} F P, \tag{4}$$

where $P\alpha$ is the preformation probability of the α particle and F and P are the average values of the normalization factor and the penetration probability, respectively:

$$F = \frac{1}{2}\int_0^\pi \frac{\sin\beta\, d\beta}{0.5 \times \int_{r_1(\beta)}^{r_2(\beta)} dr \frac{1}{\sqrt{\frac{2\mu}{\hbar^2}|Q - U_{\text{total}}(r,\beta)|}}}, \tag{5}$$

$$P = \frac{1}{2}\int_0^\pi \exp\left(-2\int_{r_2(\beta)}^{r_3(\beta)} \sqrt{\frac{2\mu}{\hbar^2}|Q - U_{\text{total}}(r,\beta)|dr}\right) \times \sin\beta\, d\beta. \tag{6}$$

The α-decay half-life is related to the decay width by the well-known expression [18]

$$T_{1/2} = \frac{\hbar \ \ln 2}{\Gamma}. \tag{7}$$

III. RESULTS AND DISCUSSION

Figure 1 shows the total potentials $\lambda(\beta)\ U_{\text{N}} + U_{\text{C}}$ for the decay of ${}_{114}\text{Ee}^{286} \to {}_{112}\text{Ec}^{282} + \alpha$ at the orientation angles $\beta = 0^{\text{o}}$ and $\beta = 90^{\text{o}}$ of the deformed daughter. The factor $\lambda(\beta)$ has value less than 1.0 and depends strongly on the emission angle β and also on both the sign and the value of the deformation parameter and it affects the inner and the barrier regions of the total potential. Table I presents a set of values of $\lambda(\beta)$ for different emission angles and different hypothetical values of the deformation parameters δ_2 and δ_4 for $G = 20$ and $L = 0$. As shown in Table I, the value of $\lambda(\beta)$ increases with the emission angles for positive δ_2 and vice versa. The wide range of variation of λ with the emission angle in most decays suggests that it would be better if λ is taken with its specific value at each angle, as given by Eq. (3). This can be justified if we assume that each decay through emission angle β is a separate event [27].

Ren *et al.* [18] determined the strength of the nuclear potential λ, used in Eq. (1); at each distance r and its average value over all orientation angles $\lambda = 0.58$ [17],

$$\frac{1}{2}\int_{r_1(\beta)}^{r_2(\beta)}\int_0^\pi \sqrt{\frac{2\mu}{\hbar^2}|Q - U_{\text{total}}(r,\beta)|}\ \sin(\beta)\, dr\, d\beta = (G - L + 1)\frac{\pi}{2}, \tag{8}$$

which means that, they used one value of λ for all emission angles and not a specific λ value for each emission angle. We label the α-decay half-life obtained from Eq. (8) by T_1, and that obtained by using the value of $\lambda(\beta)$ *at each emission angle* β, average half-lives, by T_2.

Table II presents a comparison between the two above-mentioned methods, the half-lives T_1 and T_2 are calculated for 83 deformed heavy and superheavy α-decay nuclei having Z in the range 82–118 with neutron number $N > 126$. We restrict our study to the ground-state α transitions of even-even nuclei in which the angular momentum of the α particle is zero [24], that is, partial half-life. For the considered reactions the α-particle preformation probability is taken to be equal to unity. The deformation parameters shown in Table II are taken from

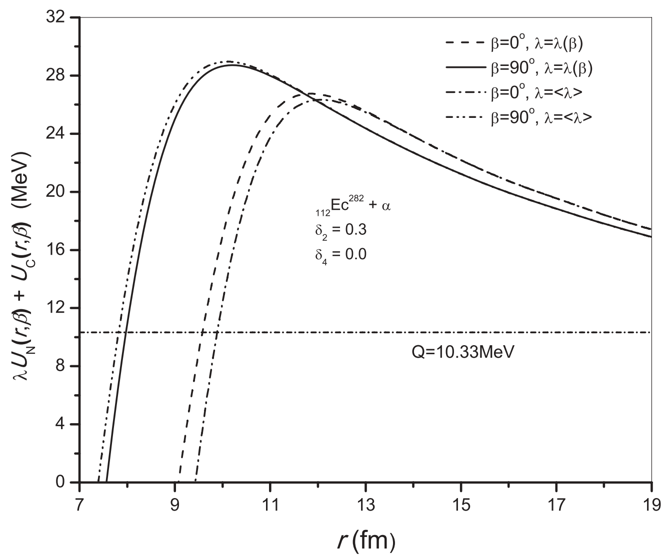

FIG. 1. Sum of the double-folding nuclear and Coulomb potentials $\lambda(\beta)\ U_{\text{N}} + U_{\text{C}}$ of the interacting pair (${}_{112}\text{Ec}^{282}$, α) for two emission angles $\beta = 0^{\text{o}}$ and $\beta = 90^{\text{o}}$ of the ${}_{112}\text{Ec}^{282}$ daughter. The average value of $\lambda = 0.58$ was obtained from Eq. (8). The values of the deformation parameters assumed are $\delta_2 = 0.3$ and $\delta_4 = 0.0$, and the Q value = 10.33 MeV.

TABLE I. Depths of the nuclear potentials $\lambda(\beta)$ of the interacting pair (${}_{112}\text{Ec}^{282}$, α) at different emission angles for different values of deformation parameters of the nucleus ${}_{112}\text{Ec}^{282}$.

β (deg)	$\lambda(\beta)$ ($\delta_2 = 0.3, \delta_4 = 0$)	$\lambda(\beta)$ ($\delta_2 = 0.3, \delta_4 = 0.1$)	$\lambda(\beta)$ ($\delta_2 = 0.3, \delta_4 = -0.1$)	$\lambda(\beta)$ ($\delta_2 = -0.3, \delta_4 = 0$)	$\lambda(\beta)$ ($\delta_2 = -0.3, \delta_4 = 0.1$)	$\lambda(\beta)$ ($\delta_2 = -0.3, \delta_4 = -0.1$)
0	0.461	0.432	0.497	0.747	0.676	0.825
20	0.478	0.462	0.497	0.710	0.680	0.743
40	0.527	0.542	0.515	0.631	0.652	0.613
60	0.592	0.609	0.577	0.558	0.572	0.547
90	0.652	0.630	0.677	0.512	0.499	0.527

TABLE II. α-decay half-lives T_1, T_2, and T_{sph} of even-even heavy and superheavy nuclei ($Z = 82$–118), in seconds, as calculated by the two different theoretical methods compared with the experimental partial half-lives for the α decay.

Parent	A_p	Q (MeV)	δ_2	δ_3	δ_4	T_{exp}	T_1 [18]	T_2 (present)	T_{sph}
$_{82}$Pb	210	3.792	−0.008	0.0	0.0	3.69×10^{16}	7.96×10^{15}	7.97×10^{15}	7.97×10^{15}
$_{84}$Po	212	8.954	0.0	−0.013	0.0	2.99×10^{-7}	1.05×10^{-7}	1.05×10^{-7}	1.06×10^{-7}
	214	7.833	0.0	0.0	0.008	1.64×10^{-4}	1.08×10^{-4}	1.08×10^{-4}	1.09×10^{-4}
	216	6.906	0.0	0.0	0.008	1.45×10^{-1}	1.25×10^{-1}	1.25×10^{-1}	1.25×10^{-1}
	218	6.115	0.009	−0.049	0.009	1.86×10^{2}	1.76×10^{2}	1.80×10^{2}	1.88×10^{2}
$_{86}$Rn	214	9.208	0.0	0.0	0.008	2.70×10^{-7}	1.29×10^{-7}	1.29×10^{-7}	1.30×10^{-7}
	216	8.2	0.0	0.0	0.008	4.50×10^{-5}	5.37×10^{-5}	5.38×10^{-5}	5.38×10^{-5}
	218	7.263	0.008	0.0	0.008	3.50×10^{-2}	4.72×10^{-2}	4.72×10^{-2}	4.73×10^{-2}
	220	6.405	0.02	−0.099	0.018	5.56×10^{1}	6.75×10^{1}	7.47×10^{1}	8.96×10^{1}
	222	5.59	0.039	−0.133	0.028	3.31×10^{5}	3.28×10^{5}	4.08×10^{5}	5.97×10^{5}
$_{88}$Ra	216	9.526	0.0	0.0	0.008	1.82×10^{-7}	1.12×10^{-7}	1.12×10^{-7}	1.13×10^{-7}
	218	8.546	0.008	0.0	0.008	2.56×10^{-5}	3.22×10^{-5}	3.23×10^{-5}	3.23×10^{-5}
	220	7.592	0.008	0.0	0.008	1.81×10^{-2}	2.40×10^{-2}	2.41×10^{-2}	2.41×10^{-2}
	222	6.679	0.04	−0.14	0.029	3.92×10^{1}	2.79×10^{1}	3.54×10^{1}	5.32×10^{1}
	224	5.789	0.111	−0.146	0.081	3.33×10^{5}	1.19×10^{5}	2.18×10^{5}	5.74×10^{5}
	226	4.871	0.137	−0.132	0.1	5.35×10^{10}	1.71×10^{10}	3.58×10^{10}	1.20×10^{11}
$_{90}$Th	218	9.849	0.008	0.0	0.008	1.09×10^{-7}	9.64×10^{-8}	9.65×10^{-8}	9.67×10^{-8}
	220	8.953	0.008	0.0	0.008	9.70×10^{-6}	1.39×10^{-5}	1.39×10^{-5}	1.39×10^{-5}
	222	8.1270	0.02	−0.085	0.01	2.05×10^{-3}	2.40×10^{-3}	2.59×10^{-3}	2.94×10^{-3}
	224	7.298	0.103	−0.144	0.072	1.33	0.43	0.72	1.64
	226	6.4509	0.13	−0.148	0.092	2.46×10^{3}	6.00×10^{2}	1.21×10^{3}	3.84×10^{3}
	228	5.5201	0.164	−0.131	0.112	8.49×10^{7}	1.42×10^{7}	3.63×10^{7}	1.56×10^{8}
	230	4.77	0.172	−0.108	0.112	3.12×10^{12}	8.13×10^{11}	1.88×10^{12}	7.69×10^{12}
	232	4.082	0.18	−0.058	0.113	5.69×10^{17}	3.00×10^{17}	6.17×10^{17}	2.06×10^{18}
$_{92}$U	220	10.3	0.008	0.0	0.008	6×10^{-8}[a]	4.42×10^{-8}	4.43×10^{-8}	4.43×10^{-8}
	222	9.5	0.008	0.0	0.008	1.40×10^{-6}	2.88×10^{-6}	2.88×10^{-6}	2.89×10^{-6}
	224	8.620	0.030	−0.118	0.019	9.4×10^{-4}	3.89×10^{-4}	4.50×10^{-4}	5.87×10^{-4}
	226	7.701	0.111	−0.138	0.081	2.69×10^{-1}	1.01×10^{-1}	1.77×10^{-1}	4.20×10^{-1}
	228	6.803	0.164	−0.135	0.112	5.75×10^{2}	9.97×10^{1}	2.33×10^{2}	9.75×10^{2}
	230	5.9927	0.173	0.0	0.111	2.67×10^{6}	1.17×10^{6}	2.06×10^{6}	4.84×10^{6}
	232	5.4136	0.182	0.0	0.112	3.20×10^{9}	1.42×10^{9}	2.63×10^{9}	6.81×10^{9}
	234	4.8577	0.198	0.0	0.115	1.09×10^{13}	3.99×10^{12}	8.01×10^{12}	2.46×10^{13}
	236	4.5731	0.207	0.0	0.108	1.00×10^{15}	4.36×10^{14}	8.92×10^{14}	2.83×10^{15}
	238	4.27	0.215	0.0	0.102	1.78×10^{17}	1.10×10^{17}	2.30×10^{17}	7.60×10^{17}
$_{94}$Pu	228	7.950	0.146	−0.127	0.1	2.00×10^{-1}[a]	6.32×10^{-2}	1.28×10^{-1}	3.91×10^{-1}
	230	7.18	0.172	0.0	0.111	1.00×10^{2}[a]	5.77×10^{1}	9.92×10^{1}	2.24×10^{2}
	232	6.716	0.191	0.0	0.114	1.71×10^{4}	3.47×10^{3}	6.51×10^{3}	1.73×10^{4}
	234	6.310	0.199	0.0	0.115	7.73×10^{5}	2.04×10^{5}	3.99×10^{5}	1.16×10^{6}
	236	5.867	0.207	0.0	0.117	1.30×10^{8}	2.89×10^{7}	5.95×10^{7}	1.91×10^{8}
	238	5.5932	0.215	0.0	0.11	3.90×10^{9}	8.70×10^{8}	1.82×10^{9}	5.98×10^{9}
	240	5.2557	0.215	0.0	0.102	2.84×10^{11}	9.44×10^{10}	1.95×10^{11}	6.21×10^{11}
	242	4.9845	0.2150	0.0	0.093	1.52×10^{13}	5.88×10^{12}	1.19×10^{13}	3.63×10^{13}
	244	4.6655	0.2240	0.0	0.0790	3.17×10^{15}	1.15×10^{15}	2.32×10^{15}	7.01×10^{15}
$_{96}$Cm	238	6.62	0.216	0.0	0.109	2.3×10^{5}[a]	5.17×10^{4}	1.07×10^{5}	3.37×10^{5}
	240	6.398	0.215	0.0	0.11	3.30×10^{6}	5.14×10^{5}	1.07×10^{6}	3.44×10^{6}
	242	6.216	0.215	0.0	0.102	1.90×10^{7}	4.00×10^{6}	8.15×10^{6}	2.52×10^{7}
	244	5.902	0.223	0.0	0.087	7.48×10^{8}	1.69×10^{8}	3.43×10^{8}	1.03×10^{9}
	246	5.475	0.224	0.0	0.071	1.82×10^{11}	5.06×10^{10}	9.91×10^{10}	2.78×10^{11}
	248	5.162	0.224	0.0	0.062	1.43×10^{13}	4.98×10^{12}	9.58×10^{12}	2.60×10^{13}
$_{98}$Cf	240	7.719	0.215	0.0	0.102	9.09×10^{1}	1.46×10^{1}	2.90×10^{1}	8.33×10^{1}
	242	7.517	0.215	0.0	0.093	2.62×10^{2}	8.34×10^{1}	1.62×10^{2}	4.44×10^{2}
	244	7.329	0.224	0.0	0.087	1.55×10^{3}	4.01×10^{2}	7.92×10^{2}	2.25×10^{3}
	246	6.862	0.224	0.0	0.079	1.62×10^{5}	3.46×10^{4}	6.77×10^{4}	1.88×10^{5}
	248	6.361	0.234	0.0	0.073	3.54×10^{7}	6.41×10^{6}	1.30×10^{7}	3.85×10^{7}
	250	6.128	0.234	0.0	0.057	4.88×10^{8}	1.05×10^{8}	2.03×10^{8}	5.55×10^{8}
	252	6.217	0.235	0.0	0.04	1.02×10^{8}	3.90×10^{7}	7.21×10^{7}	1.80×10^{8}

TABLE II. *(Continued.)*

Parent	A_p	Q (MeV)	δ_2	δ_3	δ_4	T_{exp}	T_1 [18]	T_2 (present)	T_{sph}
	254	5.927	0.225	0.0	0.03	2.04×10^9	1.48×10^9	2.59×10^9	5.89×10^9
$_{100}$Fm	246	8.374	0.224	0.0	0.079	1.55×10^0	5.01×10^{-1}	9.55×10^{-1}	2.49×10^0
	248	8.002	0.234	0.0	0.073	4.56×10^1	8.08×10^0	1.58×10^1	4.34×10^1
	250	7.557	0.234	0.0	0.057	2.28×10^3	3.70×10^2	7.01×10^2	1.80×10^3
	252	7.153	0.235	0.0	0.04	1.09×10^5	1.63×10^4	2.99×10^4	7.23×10^4
	254	7.308	0.245	0.0	0.026	1.37×10^4	3.56×10^3	6.46×10^3	1.55×10^4
	256	7.027	0.236	0.0	0.015	1.35×10^5	5.80×10^4	9.98×10^4	2.20×10^5
$_{102}$No	252	8.550	0.235	0.0	0.049	4.18×10^0	7.88×10^{-1}	1.45×10^0	3.48×10^0
	254	8.226	0.235	0.0	0.033	7.14×10^1	9.94×10^0	1.76×10^1	3.99×10^1
	256	8.581	0.245	0.0	0.018	3.64×10^0	0.628×10^0	1.1×10^0	2.43×10^0
	258	8.151	0.237	0.0	0.008	1.2×10^2 [a]	1.83×10^1	3.07×10^1	6.42×10^1
$_{104}$Rf	256	8.930	0.236	0.0	0.024	2.02×10^0	3.11×10^{-1}	5.38×10^{-1}	1.17×10^0
	258	9.250	0.246	0.0	0.011	9.23×10^{-2}	3.20×10^{-2}	5.49×10^{-2}	1.18×10^{-1}
	260	8.901	0.237	0.0	−0.001	1.0[a]	3.86×10^{-1}	6.29×10^{-1}	1.27×10^0
$_{106}$Sg	260	9.92	0.247	0.0	−0.007	9.5×10^{-3}	2.39×10^{-3}	3.93×10^{-3}	8.01×10^{-3}
	266	8.76	0.229	0.0	−0.037	25.7	6.47	9.70	1.81×10^1
$_{108}$Hs	264	10.591	0.239	0.0	−0.0250	8.5×10^{-4}	2.31×10^{-4}	3.57×10^{-4}	6.71×10^{-4}
	266	10.336	0.229	−0.036	−0.029	2.3×10^{-3}	9.49×10^{-4}	1.47×10^{-3}	2.76×10^{-3}
	270	9.02	0.23	−0.061	−0.019	3.6	3.72	6.37	14.1
$_{110}$Ds	270	11.2	0.23	0.0	−0.061	1.0×10^{-4}	3.64×10^{-5}	5.20×10^{-5}	9.28×10^{-5}
	280	9.3 [24]	0.164	0.0	−0.063	11.0 [5]	4.4	5.5	8.03
$_{112}$Ec	284	9.349	0.108	0.0	−0.028	9.8	31.0	34.7	28.9
$_{114}$Ee	286	10.33	0.089	0.0	−0.012	0.26	147×10^{-3}	159×10^{-3}	202×10^{-3}
	288	10.08	0.089	0.0	−0.029	0.8	0.72	0.78	0.94
$_{116}$Eg	290	11.00	−0.096	0.0	−0.035	7.1×10^{-3}	1.29×10^{-2}	1.38×10^{-2}	1.56×10^{-2}
	292	10.8	0.053	0.0	−0.023	18×10^{-3}	43.7×10^{-3}	45×10^{-3}	47.4×10^{-3}
118	294	11.81	0.072	0.0	− 0.031	8.9×10^{-4}	6.26×10^{-4}	6.62×10^{-4}	7.22×10^{-4}

[a]Data taken from Ref. [30].

Moller *et al*. [28]. We take the latest values of experimental partial half-lives and decay energies mainly from Ref. [29] and references therein; otherwise the reference is stated in Table II, for example, Ref. [30]. In Table II, the experimental values of the half-lives are listed first, followed by the theoretical values of T_1 [18], then the values of T_2, and next to them the half-life times for the corresponding spherical daughter nuclei. The table shows that the lifetimes of the spherical daughter nuclei, T_{sph}, are always longer than the corresponding half-lives T_1 and T_2. A simple explanation for this behavior is as follows: The deformation is reflected in β-dependent nuclear radius, which leads to enhanced penetration for larger radii and reduced penetration for smaller radii. Owing to the exponential dependence of the half-life on the penetration factor, the half-life is reduced for deformed nuclei compared to the spherical nuclei. The effect of different values of λ on the height of the barrier are shown in Fig. 1.

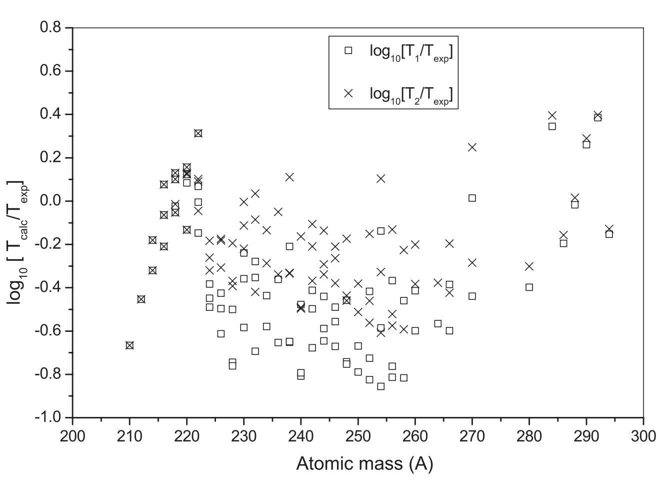

FIG. 2. Logarithms of the ratios (T_{calc}/T_{exp}) for the two different methods of calculation.

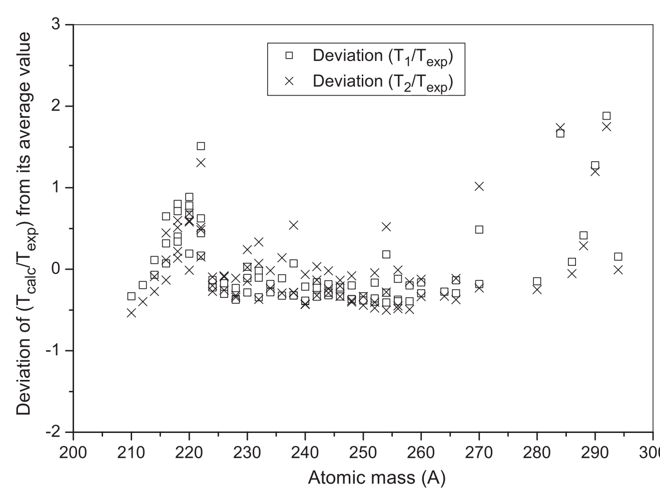

FIG. 3. Deviations of the ratios T_{calc}/T_{exp} from their average values for the two different methods of calculation.

TABLE III. Statistical values of the data in Table II.

	T_1 [18]	T_2 (present)	T_{sph}
Standard deviations ($\langle\sigma\rangle$ of the 83 α emitters)	0.4979	0.3055	0.2576
The factor 10^{σ}	3.1471	2.0205	1.8097
Average value of T/T_{exp} (preformation factor)	0.5466	0.7507	1.4756

The ratio $\frac{T_i}{T_{sph}}(i = 1, 2)$ depends on the values of the deformation parameters. For ^{226}Ra where the deformation parameters have the values $(\delta_2, \delta_3, \delta_4) = (0.137, -0.132, 0.1)$, $\frac{T_i}{T_{sph}} =$ 0.14 and 0.30 for $i = 1$ and 2, respectively. For ^{230}U where $(\delta_2, \delta_3, \delta_4) = (0.173, 0.0, 0.111)$, $\frac{T_i}{T_{sph}}$ 0.24 and 0.43 for $i =$ 1 and 2, respectively. For small values of the deformation parameters the ratio becomes equal to unity, as in the case of Po isotopes. To measure the goodness of the agreement between the experimental and theoretical half-lives, we calculate the rms error of the decimal logarithm using

$$\sigma_i = \sqrt{\frac{1}{N}\sum_{k=1}^{N}\left[\log_{10} T_{exp}^{k} - \log_{10} T_i^{k}\right]^2} \quad i = 1, 2, \qquad (9)$$

while the corresponding factor of the average absolute deviation is defined as 10^{σ_i}. In Table III, we calculated the average values of T_i/T_{exp}, $i = 1, 2$ for each one of the two methods. The average values of the preformation factors are 0.547, 0.751, and 1.476 for T_1, T_2, and T_{sph}, respectively. Figure 2 represents the variation of the logarithmic ratio for each method $\{\log(T_i/T_{exp})\}$ with the mass numbers of the 83 parent nuclei considered in the present work. The figure shows that most of the points representing $\log(T_1/T_{exp})$ spread between the two values -0.85 and 0.4 . Figure 3 represents the mass number variation of the deviations of T_i/T_{exp} from its average value for the two methods.

Here we briefly evaluate our overall calculations from the experimental half-life values of 83 nuclei, shown in Table III; the estimated standard deviations of the results of the two methods are 0.498 and 0.306, respectively, corresponding to the absolute deviations of half-lives with factors of 3.15 and 2.02. This demonstrates that method 2 is a development of method 1 [18], giving a good description of α-decay half-lives. The conclusion is that considering a specific depth of the nuclear potential at each emission angle produces the half-lives more correctly than considering an average unique value over the all emission angles.

[1] I. Tonozuka and A. Arima, Nucl. Phys. A **323**, 45 (1979).
[2] Ren Zhong-zhou and Xu Gong-ou, Phys. Rev. C **36**, 456 (1987).
[3] H. Horiuchi, Nucl. Phys. A **522**, 257c (1991).
[4] P. E. Hodgeson and E. Betak, Phys. Rep. **374**, 1 (2003).
[5] G. Audi,O. Bersillon, J. Blachot, and A. H. Wapstra, Nucl. Phys. A **729**, 3 (2003).
[6] T. N. Ginter *et al.*, Phys. Rev. C **67**, 064609 (2003).
[7] F. A. Danevich *et al.*, Phys. Rev. C **67**, 014310 (2003); G. Gan *et al.*, Eur. Phys. J. A **20**, 385 (2004).
[8] G. Gamow, Z. Phys. **51**, 204 (1928); E. U. Condon and R. W. Gurney, Nature (London) **122**, 439 (1928).
[9] N. Rowley, G. D. Jones, and M. W. Kermode, J. Phys. G **18**, 165 (1992).
[10] K. Varga, R. G. Lovas, and R. J. Liotta, Phys. Rev. Lett. **69**, 37 (1992).
[11] S. A. Gurvitz and G. Kalbermann, Phys. Rev. Lett. **59**, 262 (1987).
[12] P. Mohr, Phys. Rev. C **73**, 031301(R) (2006); D. N. Basu, Phys. Lett. B **566**, 90 (2003).
[13] B. A. Brown, Phys. Rev. C **46**, 811 (1992).
[14] Y. K. Gambhir, A. Bhagwat, and M. Gupta, Phys. Rev. C **71**, 037301 (2005).
[15] Dongdong Ni and Zhongzhou Ren, Phys. Rev. C **80**, 051303(R) (2009); **81**, 024315 (2010); **83**, 067302 (2011).
[16] Chang Xu and Zhongzhou Ren, Nucl. Phys. A **760**, 303 (2005); **753**, 174 (2005).
[17] M. Ismail, A. Y. Ellithi, M. M. Botros, and A. Adel, Phys. Rev. C **81**, 024602 (2010).
[18] C. Xu and Z. Ren, Phys. Rev. C **74**, 014304 (2006); **73**, 041301(R) (2006).
[19] R. E. Langer, Phys. Rev. **51**, 669 (1937).
[20] G. R. Satchler and W. G. Love, Phys. Rep. **55**, 183 (1979); A. M. Kobos, B. A. Brown, P. E. Hodgson, G. R. Satchler, and A. Budzanowski, Nucl. Phys. A **384**, 65 (1982).
[21] G. Bertsch, J. Borysowicz, H. McManus, and W. G. Love, Nucl. Phys. A **284**, 399 (1977).
[22] M. J. Rhoades-Brown *et al.*, Z. Phys. A **310**, 287 (1983).
[23] M. Ismail, A. Y. Ellithi, and F. Salah, Phys. Rev. C **66**, 017601 (2002); M. Ismail and W. M. Seif, *ibid.* **81**, 034607 (2010); M. Ismail, W. M. Seif, and M. M. Botros, Nucl. Phys. A **828**, 333 (2009).
[24] G. Audi, A. H. Wapstra, and C. Thibault, Nucl. Phys. A **729**, 337 (2003).
[25] B. Buck, J. C. Johnston, A. C. Merchant, and S. M. Perez, Phys. Rev. C **53**, 2841 (1996).
[26] D. Ni and Z. Ren, Phys. Rev. C **81**, 064318 (2010); P. Mohr, *ibid.* **61**, 045802 (2000).
[27] Sham K. Arun, Raj K. Gupta, Shefali Kanwar, BirBikram Singh, and Manoj K. Sharma, Phys. Rev. C **80**, 034317 (2009).
[28] P. Möller, J. R. Nix,W. D. Myers, and W. J. Swiatecki, At. Data Nucl. Data Tables **59**, 185 (1995).
[29] D. Ni and Z. Ren, Nucl. Phys. A **825**, 145 (2009), and references therein.
[30] Basudeb Sahu, Phys. Rev. C **78**, 044608 (2008), and references therein.